4–Arylbenzenesulfonamides as human carbonic anhydrase inhibitors (hCAIs): synthesis by Pd nanocatalyst–mediated Suzuki–Miyaura reaction, enzyme inhibition and X–ray crystallographic studies

Benedetta Cornelio,[a,b] Marie Laronze–Cochard,[a] Mariangela Ceruso,[c] Marta Ferraroni,[c] Graham A. Rance,[d] Fabrizio Carta,[c] Andrei N. Khlobystov,[d,e] Antonella Fontana,[b] Claudiu T. Supuran,*[,c,f] and Janos Sapi*[,a]

[a] Institut de Chimie Moléculaire de Reims, CNRS UMR 7312, Université de Reims Champagne–Ardenne, UFR Pharmacie, 51 Rue Cognacq–Jay, F–51096 Reims Cedex, France

[b] Dipartimento di Farmacia, Università "G. d'Annunzio", Via dei Vestini, I–66100 Chieti, Italy

[c] Dipartimento di Chimica Ugo Shiff, Università degli Studi di Firenze, Via della Lastruccia 3, I–50019 Sesto Fiorentino (Firenze), Italy

[d] School of Chemistry, University of Nottingham, University Park, Nottingham, NG7 2RD, UK

[e] Nottingham Nanotechnology and Nanoscience Centre, University of Nottingham, University Park, Nottingham, NG7 2RD, UK

[f] Neurofarba Dept., Università degli Studi di Firenze, Via U. Schiff 6, I–50019 Sesto Fiorentino (Firenze) , Italy

Abstract Benzenesulfonamides bearing various substituted (hetero)aryl rings in the *para*–position were prepared by palladium nanoparticle–catalyzed Suzuki–Miyaura cross–coupling reactions and evaluated as human carbonic anhydrase (hCA) inhibitors against isoforms hCA I, hCA II, hCA IX and hCA XII. Almost all of the prepared 4–arylbenzenesulfonamides showed low inhibition against hCA I isoform, whereas the other cytosolic isoenzyme, hCA II was strongly affected. The major part of these new derivatives was potent inhibition of the tumor–associated hCA XII isoform. An opposite trend was observed for phenyl (**4a**), naphthyl (**4d**) and various heteroaryl (**4p, 4q, 4s, 4w** and **4x**) substituted benzenesulfonamides which displayed sub–nanomolar hCA IX inhibition whilst poorly inhibiting the other tumor–associated isoenzyme hCA XII. The inhibition potency and

influence of the partially restricted aryl–aryl bond rotation on the activity/selectivity were rationalized by means of X–ray crystallography of the adducts of hCA II with several 4–arylbenzenesulfonamides.

Keywords*:* human carbonic anhydrases, 4–arylbenzenesulfonamides, Suzuki–Miyaura cross–coupling reactions, palladium nanoparticles, carbon nanotubes

***Corresponding Authors:** Tel: +33 (0)326 918022; fax: +33 (0)326 918029; e–mail address: janos.sapi@univ-reims.fr (JS); Tel: +39 055 4573005; fax: +39 055 4573385; e–mail address: claudiu.supuran@unifi.it (CTS)

1. Introduction

Carbonic anhydrases (CAs, EC 4.2.1.1) are metalloenzymes present in most living organisms encoded by six genetically distinct families, the human α–, the β–, γ–, δ–, ζ– and the recently reported η–CAs.[1] They catalyze the reversible hydration of carbon dioxide to the bicarbonate ion and a proton,[2-3] a simple but essential reaction involved in respiration, electrolyte secretion, biosynthesis of several important molecules (urea, lipids, glucose, etc.), pH homeostasis and tumorigenicity,[4,5] and are thus targets for the design of activators and inhibitors. In humans, activators find their pharmacological application in pathologies connected with learning and memory impairment,[3,4,6,7] whilst inhibitors, originally used as diuretics, antiglaucoma agents or antiepileptics, are more recently further employed as antiobesity agents, antitumor drugs or diagnostic tools.[3,4,6-12] In fact, the multiple pharmacological applications of CA inhibitors (CAIs) may be explained by the high number of isoforms and by their up– and down–regulation related to different pathologies. Humans express fifteen CA isoforms (hCAs), all containing a Zn(II) ion within the active site, but differing by their cellular localization (mitochondria, cytosol, cell membrane), tissues distribution and catalytic/inhibition features.[4-10,13] Even if the physiological role of relevant CAs in diverse pathologies is more and more precisely identified, one of the main difficulties concerning the development of selective inhibitors is how to manage off–target isoenzyme inhibition. Indeed, the active site of most CA isoenzymes is a rather large conical cavity where the Zn(II) ion is positioned at the bottom with two adjacent halves (one hydrophobic and one hydrophilic) and variability between isoforms is mainly observed on the edge/entrance of the active site.[13]

Disruption of the catalytic process occurs following several possible mechanisms: the inhibitor can (i) bind directly to the zinc ion,[4,14-17] (ii) anchor to the zinc–coordinating water molecule/hydroxide ion,[18-22] or (iii) bind further away from the metal ion.[23,24] Zinc–binding drugs are widely investigated as inhibitors and the sulfonamide function, following the discovery of the exceptional

CA inhibitory activity of sulfanilamide,[25] represents one of the most potent zinc–binding group (ZBG).[26-28] Several primary sulfonamide derivatives, such as acetazolamide, methazolamide, ethoxzolamide, sulthiame, diclofenamide, dorzolamide, brinzolamide, sulpiride and zonisamide, have been developed and introduced in clinical use as diuretics, antiglaucoma, neuroleptic or antiepileptic agents (Supporting Information S1).

Structural characterization of benzenesulfonamides in complex with hCAs showed that the sulfonamide function, in its deprotonated form at physiological pH, binds to the active site with coordination of the negatively charged nitrogen atom to the Zn(II) ion.[4,27] Additionally, an extended network of hydrogen bonds involving residues Thr199 and Glu106 (conserved in all α–CAs) stabilizes the binding, whilst the phenyl ring participates in van der Waals interactions with other amino acid residues within the enzyme active site.[4,13,29-31] Therefore, the binding mode of this pharmacophore appears quite similar, irrespective of the isoforms, making the rational design of isoenzyme–specific benzenesulfonamides CAIs a challenging program for medicinal chemists.[32] However, depending on the phenyl substituent (tail or linker moiety), more specific interactions can be established within the typical enzyme bipolar architecture, towards the middle part of the active site or towards its edge (Figure 1).[4,13]

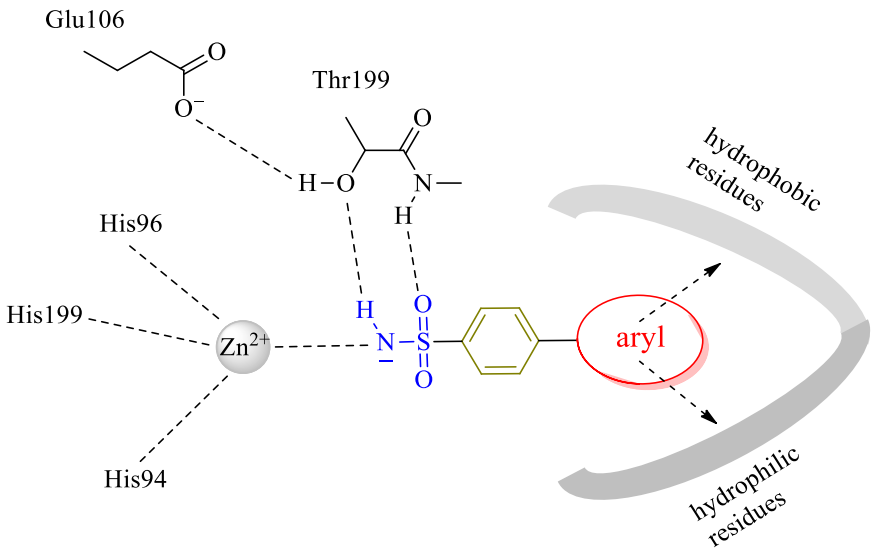

Figure 1. Exemplified representation of the binding mode of 4–arylbenzenesulfonamides at physiological pH (7.4) with the active site of hCAs. The tail (aryl) interacts with hydrophobic or hydrophilic residues depending on its nature.

Herein, we report the synthesis of new 4–arylbenzenesulfonamide derivatives by using the so–called "tail approach", a drug design strategy based on appending scaffolds (tails) of different size, shape or nature to a ZBG containing pharmacophore,[4,13,31,33-36] as opposed to the "ring approach" exploring several aromatic/heterocyclic fragments on which the ZBG is bound.[4,13,36,37] This modulation, based on the extension of benzenesulfonamide moiety by anchoring tails has been poorly investigated to date. The preparation of CAIs reported here was carried out by palladium mediated Suzuki–Miyaura cross–coupling reactions. Inhibition activity of the synthesized compounds was measured on tumor–associated isoenzymes hCA IX and hCA XII and on the physiologically dominant off–target isoforms hCA I and hCA II. To rationalize our drug design strategy, X–ray crystallography of several hCA II–sulfonamide adducts were also investigated.

2. Results and discussion

Inhibitor Design. The benzenesulfonamide scaffold is known for its inhibitory potency against CAs and 2–substituted, 2,4–disubstituted and 3,4–disubstituted derivatives were shown in many cases to act as weaker inhibitors compared to 4–substituted derivatives.[4] Up until now, according to the "tail approach", esters, amides, imines, urea and thiourea functions were commonly used linkers to covalently attach the tail fragment to the benzene ring.[4,26,27] This approach gives higher flexibility to molecules but requires multi–step chemical pathways to obtain the desired compounds. The rationale for our drug design strategy was, on the contrary, the extension of the benzene–ZBG pharmacophore by anchoring an aryl moiety as a tail directly to the *para* position of the benzene ring, in the absence of any additional linker. This straightforward single–step approach, was

realized by using palladium catalyzed Suzuki–Miyaura cross–couplings of a unique aryl halide, 4–iodobenzenesulfonamide **2**, with a series of aryl boronic acids or esters **3a**–**x** (Scheme 1 and Supporting Information, Table S1). In fact, this reaction represents a very efficient method for the formation of new carbon–carbon bonds,[38] applicable to a wide range of aryl halides and boronic acids and esters[39] and hereupon can be further exploited for the synthesis of molecules of biological interest.[40,41] In this study, we prepared a library of twenty four new 4–arylbenzenesulfonamides (Figure 2) in which a high chemical diversity was guaranteed by a large spectrum of commercially available boronic acids or esters. An additional key structural element for a more efficient enzyme–inhibitor interaction of the biaryl moiety was represented by the finely tunable torsion angle derived from electrostatic interactions and/or steric repulsions. To the best of our knowledge such biaryl systems have not been investigated as potential CA inhibitors. Depending on the interactions with the active site, our new 4–arylbenzenesulfonamide derivatives can be classified into four families. Compounds **4a**–**d** are ZBG–benzene–hydrophobic ring scaffolds able to interact with the hydrophobic region of the enzyme. Compounds **4e**–**k** belong to a large family whose tails possess functionalities able to establish hydrogen bonds with the hydrophilic half. Trisaryl sulfonamides **4l**–**n** constitute a further class of molecules, designed to explore deep regions within the enzyme. Finally, derivatives **4o**–**x** allow investigation of both hydrophobic interactions of the heterocyclic moiety and the additional role of hydrogen bonding of the heteroatoms with the enzyme active site.

Chemistry. 4–Iodobenzenesulfonamide **2** was obtained by an amidification reaction of the corresponding sulfonylchloride[42] (Supporting Information, S3 and Scheme S1) while all boronic acids or esters **3a**–**x** were commercially available. In a previous study,[43] we explored the preparation (Supporting Information, S2 and Figure S2) and catalytic properties of a new heterogeneous catalyst comprising palladium nanoparticles stabilized by dodecanethiol and adsorbed on multi–walled carbon nanotubes (MWNT/PdNP@$SC_{12}H_{25}$). This composite material

displayed attractive catalytic function, exhibiting exemplary activity at lower catalytic loadings in comparison to classical homogeneous palladium complexes and excellent recyclability, showing good performance up to five catalytic cycles. Moreover, due to the heterogeneity of the catalytic system, this nanomaterial was easily removed from the reaction medium by a simple filtration. As a test reaction, coupling of **2** with phenylboronic acid **3a** was therefore carried out using both the homogeneous palladium catalyst $PdCl_2(dppf)\cdot CH_2Cl_2$ and the heterogeneous nanocatalyst MWNT/PdNP@$SC_{12}H_{25}$ (Supporting Information, Table S1). The desired cross−coupled product **4a** was obtained in only 56% yield using the $PdCl_2(dppf)\cdot CH_2Cl_2$ catalyst while near quantitative yield (97%) was observed for the same reaction catalyzed by the more performant MWNT/PdNP@$SC_{12}H_{25}$ catalyst. Moreover, the high chemical yield achieved in the case of heterogeneous nanocatalyst is significant;−sulfonamides obtained by traditional homogeneous catalysis often require additional purification by column chromatography, whereas the cross−coupling reaction using MWNT/PdNP@$SC_{12}H_{25}$ afforded compound **4a** in pure form directly by crystallization from the reaction mixture after removal of the catalyst by filtration and subsequent solvent evaporation. In view of these improvements in synthetic approach, we decided to apply the MWNT/PdNP@$SC_{12}H_{25}$ nanocatalyst to the synthesis of all novel sulfonamides in this study. We prepared twenty four 4−arylbenzenesulfonamides coupling boronic acids or esters possessing electron withdrawing or electron donating groups and substituted at the *ortho*, *meta* or *para* positions (Supporting Information, Table S1). The products of the cross−coupling reactions were obtained in a range of yields from 56% to 98% (Figure 2 and Supporting Information, Table S1) illustrating the improved performance and versatility of this catalyst and its compatibility with heteroaromatic scaffolds. Indeed, only compounds **4o** and **4p**, obtained from the reaction with less reactive boronic acids **3o** and **3p**, were isolated in lower yields and required long reaction time as compared to the more reactive substrates (Supporting Information, Table S1). A long reaction time was also required for cross−couplings with sterically hindered *ortho*-substituted boronic acids **3b**,

3c and **3t** (Supporting Information, Table S1) but the corresponding products were isolated in good yields, confirming the efficiency of our heterogeneous catalyst in different experimental conditions.

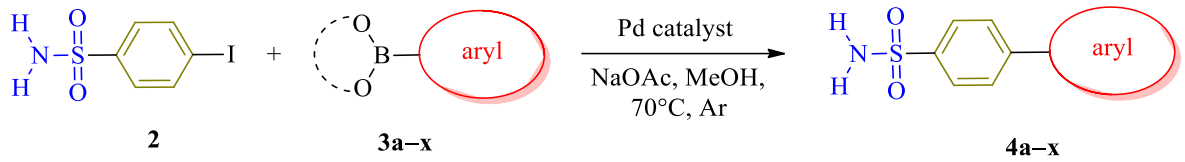

2 **3a–x** **4a–x**

Scheme 1. Synthesis of 4–arylbenzenesulfonamides **4a**–**x** using the palladium–catalyzed Suzuki–Miyaura cross–coupling reaction of 4–iodobenzenesulfonamide **2** and boronic acids or esters **3a**–**x**.

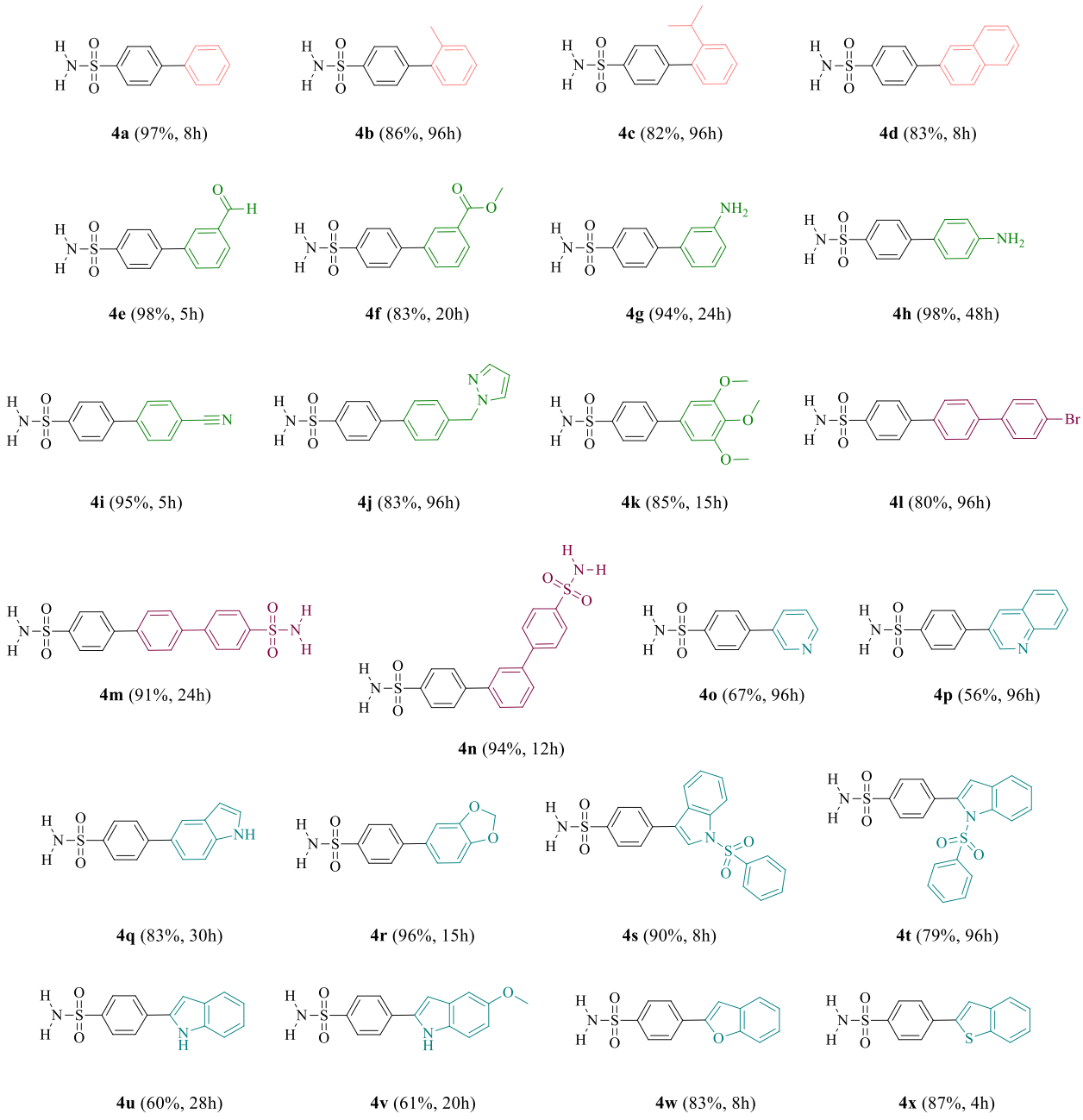

Figure 2. Structures of 4–arylbenzenesulfonamides **4a**–**x**, yields of isolated products and reaction time required for the cross–coupling reactions catalyzed by MWNT/PdNP@$SC_{12}H_{25}$.

CA inhibition. Inhibition data with the new group of benzenesulfonamides **4a**–**x** reported here, against the human (h) cytosolic CA isoforms hCA I and hCA II and transmembrane and tumor–associated isoforms hCA IX and hCA XII are shown in Table 1 and compared to the inhibitory activity of the standard sulfonamide inhibitor acetazolamide (**AAZ**). The structure–activity relationships (SARs) can thus be summarized as follows.

(i) The cytosolic and ubiquitous isoform hCA I was poorly inhibited by the majority of the compounds reported in this current study which exhibited K_Is in a micromolar range (1–9.5 μM). Only derivatives **4c** and **4s** were between 2 and 3 times more potent than **AAZ**, with K_Is of 146 and 83.6 nM respectively and compounds **4a**, **4p** and **4q** were rather effective hCA I inhibitors, possessing K_I values in a nanomolar range (24.5–41.5 nM) and thus inhibition potency between 6 and 10 folds higher compared to that obtained by the standard drug acetazolamide (K_{IAAZ} = 250 nM). On the contrary, derivatives **4l**–**n**, **4r** and **4t** did not show any inhibitory activity up to 10 μM concentration, whereas compounds **4u**, **4w** and **4x** only moderately inhibited hCA I isoform, possessing inhibition constants in the range of 184.7–656 nM, similar to that of the clinically used agent **AAZ**. The low inhibition of this new series of benzenesulfonamide compounds against the mentioned human CA isoenzyme may represent a positive and interesting feature, since the ubiquitous isoform hCA I, which is abundant in red blood cells, can be certainly considered an important off–target when research of CAIs antitumor agents is involved.[44,45]

(ii) Most of benzenesulfonamides investigated in our study behaved as very strong and effective inhibitors of the second cytosolic and physiologically dominant isoform hCA II, with K_Is in sub–nanomolar/nanomolar range between 0.68 and 19.1 nM, except for compounds **4l**–**n** and **4v** which, possessing K_Is in the range of 324–764 nM, were low potency inhibitors. Therefore, they were generally found to be similar or slightly better hCA II inhibitors compared to **AAZ** (K_I = 12 nM). Although these compounds possess a rather extensive molecular diversity, SAR is almost impossible to define as all substituted moieties lead to potent inhibition of this isoform.

(iii) Derivatives **4a**, **4d**, **4p**–**q**, **4s**, **4w** and **4x** exhibited K_Is for the hCA IX isoform in the range of 0.17–0.37 nM, about two orders of magnitude lower compared to that possessed by the clinically used **AAZ** and have shown a selectivity ratio for inhibiting this transmembrane isoform over the cytosolic ones between 6 and 8 times higher with respect to **AAZ**, except for benzenesulfonamides **4d** and **4x** displaying selectivity ratios as high as 4545 and 1763 over the off–target hCA I. The

least effective hCA IX inhibitors were derivatives **4c**, **4h**–**n** and **4r**, which showed K_Is in a very narrow range of 208–276 nM, thus being low potency inhibitors of this isoform compared to the clinically used inhibitor **AAZ**. The remaining derivatives **4e**–**g**, **4o** and **4t**–**v** have exhibited moderate inhibitory potency against this isoform (K_Is values between 78.1 and 159 nM).

In the phenylsulfonylindolyl series, regioisomerism seems to play a significant role in enzyme inhibition. Indeed, **4t** displayed weaker inhibition potency against hCA IX relative to its regioisomer **4s** but K_I values similar to those of compounds **4u** and **4v**, showing that probably no specific interactions were established by the unsubstituted NH function of derivatives **4u** and **4v** with residues in enzyme active site. When the nitrogen has been replaced by an oxygen or sulfur atom such as in the benzofuranyl– and benzothienylbenzenesulfonamide derivatives **4w** and **4x**, respectively, the inhibitory activity against the transmembrane hCA IX isoform highly increased with consequently decrease of K_I values from low micromolar to sub–nanomolar range. Supposing that the heteroaryl moiety of **4u**, **4w** and **4x** has the same orientation within the active site, the improvement of inhibition may be attributed to the capacity of oxygen or sulfur atoms to establish hydrogen bonds with the protein in both hCA IX and hCA II. In the case of **4s** the same kind of hydrogen bonding may be involved with one of the two oxygens of the phenylsulfonyl group. The lipophilic character of the phenyl ring of the latter suggests a close contact with the hydrophobic half of the active site allowing the phenylsulfonyl group protected indole to occupy a binding position.

(iv) Most of compounds reported in the current study showed to be very efficient hCA XII inhibitors possessing inhibition activity mainly at low nanomolar range and therefore of the same order of magnitude of **AAZ**. Indeed, the best inhibitors, derivatives **4c** and **4e** displayed even a sub–nanomolar K_I value of 0.58 nM and compounds **4g**, **4m**, **4r** and **4u** showed inhibition potency against hCA XII isoform comparable to that of the clinically used **AAZ** with K_Is in a very narrow range of 4.3–5.6 nM. On the contrary, derivatives **4a**, **4p**, **4s** and **4v** displayed a similar and

middling potency as hCA XII inhibitors, with inhibition constants in low sub−micromolar range between 92.7 and 760 nM, whereas **4d**, **4w** and **4x** did not exhibit any inhibitory activity up to concentrations of 10 μM.

It is also important to note that this second transmembrane tumor−associated isoform, hCA XII, was inhibited by the new series of investigated benzenesulfonamides much more than the other transmembrane tumor−associated isoform, hCA IX. Indeed, the presence of a substituent in the aryl moiety (tail) at the *ortho* position, likely affecting the rotation ability of the benzenesulfonamide derivatives, appears to reduce the inhibitory activity against the hCA IX isoform and improve the inhibition potency against the hCA XII (compare, as an example, compounds **4a, 4b** and **4c**)**.** The selectivity ratio for inhibiting the target hCA XII isoform over the cytosolic and off−target hCA II for most of this series of derivatives is rather low compared to that shown by the standard **AAZ**, except for derivatives **4l**–**n**. In particular, derivative **4m** represents the best selective inhibitor of the series against the tumor−associated isoform hCA XII over the cytosolic hCA II.

We can conclude that most of the sulfonamides belonging to this new series of derivatives obtained using an innovative synthetic pathway, have shown to possess high inhibition potency against the tumor−associated target isoforms, having on the other hand good selectivity ratios over the off−target cytosolic isoforms, in particular against hCA I.

Table 1. Inhibition data of human CA isoforms hCA I, II, IX and XII with 4−arylbenzenesulfonamide drugs **4a**–**x** and the standard sulfonamide inhibitor acetazolamide (**AAZ**) by a stopped flow CO_2 hydrase assay.[46] Colors coding in the tails refers as follow: pink is indicative of hydrophobic rings (derivatives **4a**–**4d**); green refers to aryl possessing functionalities able to establish hydrogen bonds (derivatives **4e**–**4k**); magenta codes tails in trisaryl sulfonamides (derivatives **4l**–**4n**); blue relates to heteroaromatic scaffolds (derivatives **4o**–**4x**).

Drug	**Ar**	K_I^a (nM)		Selectivity^{b,c}

		hCA I	hCA II	hCA IX	hCA XII		I/IX	II/IX	I/XII	II/XII
4a		41.5	0.79	0.21	92.7		198	3.8	0.5	0.009
4b		3499	1.2	20.1	47.0		174	0.06	74.5	0.03
4c	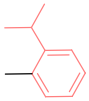	146	0.98	208	0.58		0.7	0.005	252	1.7
4d	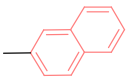	1000	0.69	0.22	/[d]		4545	3.1	/[e]	/[e]
4e	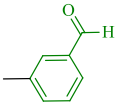	1178	2.1	98.5	0.58		12.0	0.02	2031	3.6
4f	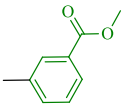	6965	14.2	159	19.5		43.8	0.09	357	0.7
4g	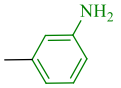	2340	9.3	126	4.3		18.6	0.07	544	2.2
4h	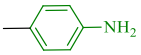	3701	12.3	235	36.5		15.7	0.05	101	0.3
4i	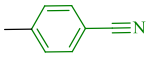	1335	1.2	228	14.2		5.9	0.005	94.0	0.08
4j	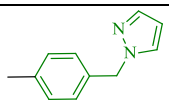	6966	11.1	216	38.3		32.3	0.05	182	0.3
4k	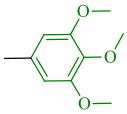	9516	19.1	259	32.2		36.7	0.07	296	0.6
4l	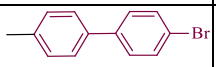	/[d]	764	224	54.2		/[e]	3.4	/[e]	14.1
4m	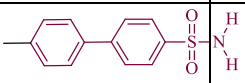	/[d]	324	240	4.9		/[e]	1.4	/[e]	66.1
4n	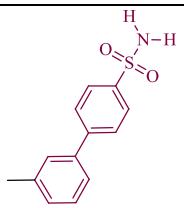	/[d]	397	276	55.6		/[e]	1.4	/[e]	7.1
4o		2397	16.6	78.1	20.3		30.7	0.2	118	0.8
4p	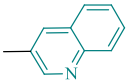	35.2	2.5	0.18	760		196	13.9	0.05	0.003
4q	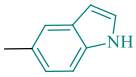	24.5	0.95	0.17	65.0		149	5.6	0.4	0.01
4r	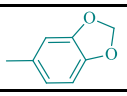	/[d]	18.0	258	5.2		40.1	0.07	1992	3.5

4s	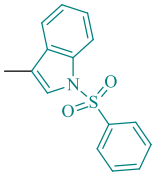	83.6	0.68	0.24	96.7		348	2.8	0.9	0.007
4t	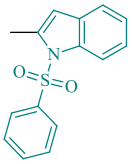	/[d]	11.7	100	33.9		229	0.1	674	0.3
4u	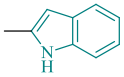	656	10.2	124	5.6		4.6	0.08	101	1.8
4v	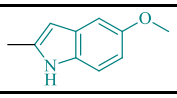	2645	764	156	415		17.0	4.9	6.4	1.8
4w	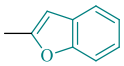	184.7	0.70	0.37	/[d]		499	1.9	/[e]	/[e]
4x	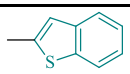	370.3	0.84	0.21	/[d]		1763	4.0	/[e]	/[e]
AAZ	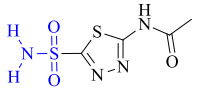	250.0	12.1	25	5.7		10.0	0.5	43.9	2.1

[a] Errors within the range of ± 5–10 % of the reported values, from 3 different assays (data not shown).[b] Selectivity ratios between K_Is of hCA I or hCA II and hCA IX. [c] Selectivity ratio between hCA I or hCA II and hCA XII. [d] Not active >10000 nM. [e] Not determined.

Crystallography. X–ray crystallography of hCA II adducts with sulfonamides **4c, 4g** and **4h** were investigated in this study (Figure 3 and Supporting Information, Table S2). At physiological pH conditions, the three inhibitors were found within the hCA II active site in the deprotonated sulfonamide form: the negatively charged nitrogen atom coordinates to the Zn(II) ion and is involved in a strong hydrogen bond with the OH group of Thr199 residue. Additionally, one of the sulfonamide oxygens establishes a hydrogen bond with the NH amide of Thr199. These strong ionic and hydrogen bond interactions are thus involved in the stabilization of the enzyme–inhibitor adducts. The three inhibitors were found in a similar conformation where the dihedral angles of the directly attached phenyl rings are close to 120° for **4c** and 45° for both **4g** and **4h**. Aminophenyl derivatives **4g** and **4h** superpose almost perfectly and the nitrogen atom of their aniline moiety establishes hydrogen bonds with two and one water molecules, respectively. Hydrophobic

interactions are observed between the aryl rings of **4g** and **4h** and residues Thr200, Leu198 and Phe131. This great similarity concerning the orientations and interactions of **4g** and **4h** *vs*. the hCA II active site may explain the close K_I values of 9.3 and 12.3 nM, respectively (Table 1). Benzenesulfonamide **4c** bearing an *ortho*– *iso*propyl group on the tail phenyl ring orients differently as compared to derivatives **4g** and **4h**. In fact, as illustrated in Figure 3, the *ortho*–*iso*propylphenyl ring system better accommodates the hydrophobic pocket as compared to the other two derivatives, establishing van der Waals interactions with both residues Phe131 and Val121. This more efficient fitting may be the origin of a higher inhibition potency of **4c** (K_I = 0.98 nM) against hCA II.

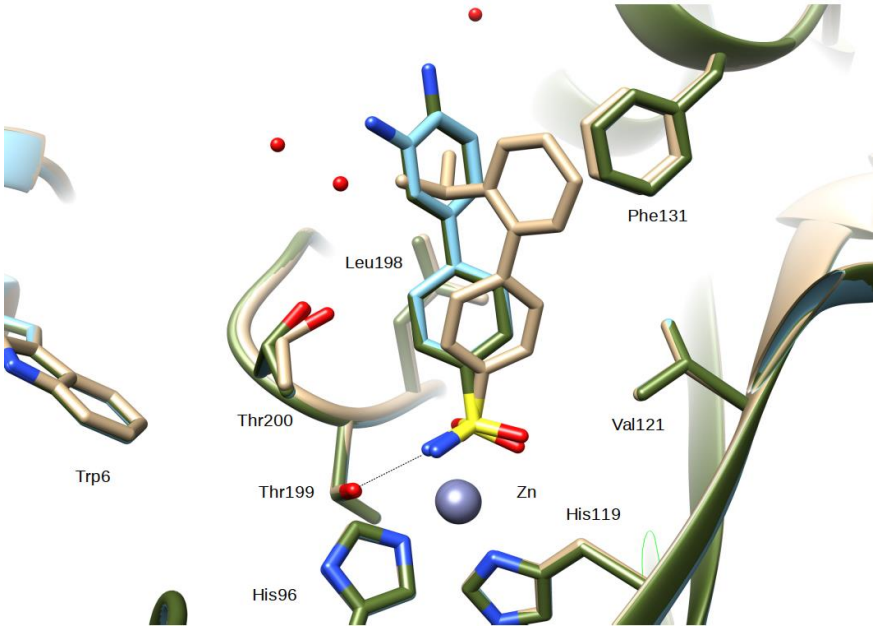

Figure 3. Superposition of sulfonamides **4c** (brown), **4g** (blue) and **4h** (green) bound to hCA II active site in the corresponding enzyme−inhibitor adducts. The sulfonamide function is depicted as sticks, the labeled Zn(II) ion is the gray sphere, two of its three ligands (His96 and 119) and residues in the binding of the inhibitors are also shown. Water molecules coordinated to the nitrogen atom of the aniline moiety are represented as red spheres.

3. Conclusion

We report~~ed~~ the preparation of a series of new 4–arylbenzenesulfonamide derivatives and their biological evaluations as carbonic anhydrase inhibitors. The so–called “tail approach” drug–design strategy was based on an efficient palladium nanoparticle~~s~~ (MWNT/PdNP@$SC_{12}H_{25}$) catalyzed Suzuki–Miyaura cross–coupling reactions allowing a wide pharmacomodulation of the aryl moiety. Enzyme inhibition assays displayed low inhibitory potency for almost the whole collection of compounds against cytosolic hCA I isoenzyme, while the other cytosolic one, hCA II, was strongly affected by most of the derivatives (except for **4l**–**4n** and **4v**). Benzenesulfonamides bearing phenyl (**4a**), naphthyl (**4d**) and some bicyclic heteroaryl (**4p**, **4q**, **4s**, **4w**, **4x**) rings showed sub–nanomolar (K_I = 0.17–0.37 nM) inhibition against the tumor–associated hCA IX isoenzyme with very high selectivity (from 382 to more than 10^5) *vs*. the other tumor–associated hCA XII isoenzyme. Most of the prepared derivatives were potent hCA XII inhibitors (K_I = 4.3-38.3 nM), comparable to the clinically used acetazolamide (**AAZ**). Bulky tails such as *ortho* and *meta* substituted phenyl rings probably affect the aryl–aryl bond rotation which may explain the high potency observed for derivatives **4c** and **4e**. X–Ray crystallography of hCA II–**4c** adduct evidenced a different active–site occupancy of **4c** within hCA II and consequently an improved inhibition activity owing to a restricted aryl–aryl bond rotation. The selectivity of the prepared compounds against the tumor–associated hCA XII *vs*. the cytosolic isoenzyme hCA II remained rather low with respect to the standard reference **AAZ** except for functionalized trisaryl derivatives. These findings shed light on the importance of the finely tunable 4–aryl substituted benzenesulfonamides as potent and selective hCA inhibitors and on the basis of these preliminary results, the design of next generation inhibitors will be engaged.

4. Experimental section

General

All solvents were of reagent grade and, when necessary, purified and dried by standard methods. All reagents were purchased from Sigma–Aldrich, Alfa Aesar and TCI and used without further purification. Carbon nanostructures – MWNT (Baytubes C150P, made by chemical vapor deposition) were obtained from Bayer Material Science and treated with concentrated hydrochloric acid prior to use to minimize the content of residual metal catalyst from synthesis (Supporting Information, S2.1). All glassware was cleaned with a mixture of hydrochloric and nitric acid (3:1 *v/v*, 'aqua regia') and rinsed thoroughly with deionized water, cleaned with potassium hydroxide in isopropyl alcohol and finally rinsed with deionized water. Reactions and products were monitored by thin layer chromatography (TLC) on silica gel (KIESELGEL 60 F_{254}, Merck). Column chromatography purifications were performed on CHROMAGEL® Silice 60 ACC 70–200 µm silica gel. Melting points were determined on a Stuart SMP3 Melting Point Apparatus (capillary tube). IR spectra were measured on a Perkin–Elmer Spectrum BX FTIR instrument. NMR spectra were recorded on a Bruker AC–300 spectrometer (^{1}H at 300 MHz and ^{13}C at 75 MHz) at 298K using DMSO–d_6 as solvent. All ^{1}H NMR and ^{13}C NMR spectra are reported in δ units (ppm) using TMS as internal standard. Coupling constants *J* are expressed as s, brs, d, dd, ddd, td, t, dt, q and m and correspond to singlet, broad singlet, doublet, doublet of doublets, doublet of doublet of doublets, triplet of doublets, triplet, doublet of triplets, quarter and multiplet, respectively. Mass spectra were recorded on a GCT Waters apparatus using ammonia chemical ionization (CI, HRMS) or electron impact ionization (EI, HRMS). Thermogravimetric analysis was performed using a TA Instruments SDT Q600 under a flow of air at a rate of 90 mL min^{-1} at a heating rate of 10 ^{o}C min^{-1} from room temperature to 1000 ^{o}C. Transmission electron microscopy (TEM) was performed using a JEOL 2100F TEM (field emission gun source, information limit < 0.19 nm) at room temperature. Analysis of nanoparticle size was conducted using Gatan DigitalMicrograph software. Energy dispersive X–ray analysis was performed using an Oxford Instruments INCA 560 X–ray microanalysis system. TEM samples were prepared by drop–drying methanolic solutions onto a copper grid

mounted “lacey” carbon films. Elemental analyses were carried out using a Perkin Elmer CHN 2400 apparatus. Purity of the final products (**4a-x**) was checked by elemental analysis (± 0.4 % of the theoretical values) and by NMR spectra (Supporting Information, S5).

General procedure for the synthesis of 4–arylbenzenesulfonamides 4a–x

4–Arylbenzenesulfonamides **4a**–**x** were prepared using the Suzuki–Miyaura cross–coupling reaction of 4–iodobenzenesulfonamides **2** with boronic acids or esters **3a**–**x** in a method analogous to that outlined in our previous study (Supporting Information, S4).[41] In a typical procedure, **2** (56.8–170.4 mg, 0.2–0.6 mmol, 1.0–2.0 eq.), **3a**–**x** (48.7–271.4 mg, 0.27–1.04 mmol, 1.3–2.6 eq.), sodium acetate (38.5–114.8 mg, 0.47–1.4 mmol, 2.3–4.6 eq.) and MWNT/PdNP@$SC_{12}H_{25}$ (2.5–7.6 mg, 2–4 mol %) were placed in a two–necked round–bottomed flask under an inert atmosphere of argon. A degassed solution of methanol (15 mL) was added *via cannula* and the resulting suspension stirred at 70 °C. After cooling to room temperature, the suspension was filtered through a PTFE membrane filter (pore diameter 0.2 μm) and the obtained filtrate concentrated to dryness. The crude solids were then recrystallized from methanol or purified by flash column chromatography on a silica gel (Supporting Information, S4).

4–(Phenyl)benzenesulfonamide (4a). White solid, 100%. mp: 226 °C. ν_{max} (KBr) / cm^{-1}: 3344 (s) (SO_2NH_2), 3251 (CH), 1295 (s) (SO_2NH_2), 1168 (s) (SO_2NH_2), 1155 (s), 1101. ^{1}H NMR (300 MHz, DMSO–d_6) δ (ppm): 7.95–7.85 (m, 4H, H–2, H–6, H–3 and H–5), 7.75 (dd, J = 7.1, 1.6 Hz, 2H, H–2′ and H–6′ or H–3′ and H–5′), 7.57–7.50 (m, 2H, H–2′ and H–6′ or H–3′ and H–5′), 7.49–7.41 (m, 1H, H–4′), 7.43 (s, 2H, SO_2NH_2). ^{13}C NMR (75 MHz, DMSO–d_6) δ (ppm): 143.6 (C), 143.2 (C), 138.9 (C), 129.3 (2 × CH), 128.6 (CH–4′), 127.4 (2 × CH), 127.2 (2 × CH), 126.5 (2 × CH). MS (EI) *m/z* (%): 233 (100, $[M]^+$), 153 (65, $[M]^+ - SO_2NH_2$), 152 (64). HRMS (EI) calcd for $C_{12}H_{11}NO_2S$ $[M]^+$ 233.0511. Found 233.0513. Anal. Calcd for $C_{12}H_{11}NO_2S$: C, 61.78; H, 4.75; N, 6.00; S, 13.75. Found: C, 61.48; H, 4.64; N, 5.98; S, 13.39.

4–(2–Methylphenyl)benzenesulfonamide (4b). White solid, 86%. mp: 157 °C. ν_{max} (KBr) / cm^{-1}: 3359 (SO_2NH_2), 3266 (CH), 1323 (s) (SO_2NH_2), 1305 (s), 1148 (s) (SO_2NH_2), 1099. ^1H NMR (300 MHz, DMSO–d_6) δ (ppm): 7.90 (d, J = 7.9 Hz, 2H, H–2 and H–6 or H–3 and H–5), 7.56 (d, J = 7.9 Hz, 2H, H–2 and H–6 or H–3 and H–5), 7.44 (s, 2H, SO_2NH_2), 7.38–7.20 (m, 4H, H–3′, H–4′, H–5′ and H–6′), 2.25 (s, 3H, CH_3). ^{13}C NMR (75 MHz, DMSO–d_6) δ (ppm): 144.9 (C), 142.8 (C), 140.1 (C), 134.9 (C), 130.7 (CH), 129.7 (CH–2 and CH–6 or CH–3 and CH–5), 129.6 (CH), 128.2 (CH), 126.3 (CH), 125.8 (CH–2 and CH–6 or CH–3 and CH–5), 20.3 (CH_3). MS (EI) *m/z* (%): 247 (99, $[M]^+$), 167 (78, $[M]^+ - SO_2NH_2$), 166 (64), 165 (100), 152 (59). HRMS (EI) calcd for $C_{13}H_{13}NO_2S$ $[M]^+$ 247.0667. Found 247.0671. Anal. Calcd for $C_{13}H_{13}NO_2S$: C, 63.13; H, 5.30; N, 5.66; S, 12.97. Found: C, 62.84; H, 5.15; N, 5.87; S, 12.71.

4–(2–*iso*–propylphenyl)benzenesulfonamide (4c). White solid, 82%. mp: 162 °C. ν_{max} (KBr) / cm^{-1}: 3339 (SO_2NH_2), 3240 (CH), 2946 (CH), 1316 (s) (SO_2NH_2), 1142 (s) (SO_2NH_2), 1096. ^1H NMR (300 MHz, DMSO–d_6) δ (ppm): 7.90 (d, J = 8.0 Hz, 2H, H–2 and H–6 or H–3 and H–5), 7.50 (d, J = 8.0 Hz, 2H, H–2 and H–6 or H–3 and H–5), 7.51–7.38 (m, 2H), 7.44 (s, 2H, SO_2NH_2), 7.28 (t, J = 7.5 Hz, 1H), 7.16 (d, J = 7.5 Hz, 1H), 2.91 (q, J = 6.8 Hz, 1H, $CH(CH_3)_2$), 1.14 (d, J = 6.8 Hz, 6H, $CH(CH_3)_2$). ^{13}C NMR (75 MHz, DMSO–d_6) δ (ppm): 145.8 (C), 145.1 (C), 142.9 (C), 139.4 (C), 129.8 (CH–2 and CH–6 or CH–3 and CH–5), 129.6 (CH), 128.6 (CH), 126.0 (CH), 125.9 (CH), 125.8 (CH–2 and CH–6 or CH–3 and CH–5), 29.3 ($CH(CH_3)_2$), 24.2 ($CH(CH_3)_2$). MS (EI) *m/z* (%): 275 (35, $[M]^+$), 195 (10, $[M]^+ - SO_2NH_2$), 180 (100), 165 (70). HRMS (EI) calcd for $C_{15}H_{17}NO_2S$ $[M]^+$ 275.0980. Found 275.0985. Anal. Calcd for $C_{15}H_{17}NO_2S$: C, 65.43; H, 6.22; N, 5.09; S, 11.64. Found: C, 65.21; H, 6.22; N, 5.25; S, 11.60.

4–(2–naphthalenyl)benzenesulfonamide (4d). White solid, 83%. mp: 266 °C. ν_{max} (KBr) / cm^{-1}: 3302 (SO_2NH_2), 3235 (CH), 1323 (s) (SO_2NH_2), 1166 (s) (SO_2NH_2), 1093. ^1H NMR (300 MHz, DMSO–d_6) δ (ppm): 8.35 (s, 1H, H–1′), 8.11–7.95 (m, 7H), 7.93 (dd, J = 8.7, 1.5 Hz, 1 H), 7.64–7.55 (m, 2H), 7.46 (s, 2H, SO_2NH_2). ^{13}C NMR (75 MHz, DMSO–d_6) δ (ppm): 143.2 (C),

143.0 (C), 136.0 (C), 133.2 (C), 132.6 (C), 128.7 (CH), 128.4 (CH), 127.6 (CH), 127.4 (2 × CH), 126.7 (2 × CH), 126.4 (2 × CH), 126.0 (CH), 125.0 (CH). MS (EI) *m/z* (%): 283 (100, $[M]^+$), 204 (56), 203 (59, $[M]^+ - SO_2NH_2$), 202 (72). HRMS (EI) calcd for $C_{16}H_{13}NO_2S$ $[M]^+$ 283.0667. Found 283.0665. Anal. Calcd for $C_{16}H_{13}NO_2S$: C, 67.82; H, 4.62; N, 4.94; S, 11.32. Found: C, 67.46; H, 4.68; N, 4.86; S, 11.18.

4–(3–formylphenyl)benzenesulfonamide (4e). White solid, 98%. mp: 116 °C. ν_{max} (KBr) / cm^{-1}: 3308 (SO_2NH_2), 3230 (CH), 1685 (s) (C=O), 1339 (s) (SO_2NH_2), 1181, 1163 (s) (SO_2NH_2), 1096. ^{1}H NMR (300 MHz, DMSO–d_6) δ (ppm): 10.13 (s, 1H, C*H*O), 8.30 (s, 1H, H–2′), 8.12 (d, J = 7.8 Hz, 1H), 8.01–7.93 (m, 5H), 7.77 (t, J = 7.8 Hz, 1H), 7.46 (s, 2H, SO_2NH_2). ^{13}C NMR (75 MHz, DMSO–d_6) δ (ppm): 193.3 (*C*HO), 143.7 (*C*–SO_2NH_2), 142.2 (C), 139.7 (C), 137.1 (C), 133.2 (CH), 130.3 (CH), 129.1 (CH), 128.5 (CH), 127.6 (CH–2 and CH–6 or CH–3 and CH–5), 126.6 (CH–2 and CH–6 or CH–3 and CH–5). MS (EI) *m/z* (%): 261 (100, $[M]^+$), 181 (32, $[M]^+ - SO_2NH_2$), 152 (99). HRMS (EI) calcd for $C_{13}H_{11}NO_3S$ $[M]^+$ 261.0460. Found 261.0465. Anal. Calcd for $C_{13}H_{11}NO_3S$: C, 59.76; H, 4.24; N, 5.36; S, 12.27. Found: C, 59.84; H, 4.05; N, 5.26; S, 12.40.

4–(3–methoxycarbonylphenyl)benzenesulfonamide (4f). White solid, 83%. mp: 177 °C. ν_{max} (KBr) / cm^{-1}: 3333 (SO_2NH_2), 3245 (CH), 1716 (s) (C=O), 1326 (s) (SO_2NH_2), 1248, 1179 (s) (SO_2NH_2), 1083. ^{1}H NMR (300 MHz, DMSO–d_6) δ (ppm): 8.27 (t, J = 1.7 Hz, 1H, H–2′), 8.08–8.01 (m, 2H), 7.95 (brs, 4H, H–2, H–3, H–5 and H–6), 7.70 (t, J = 7.8 Hz, 1H, H–5′), 7.47 (s, 2H, SO_2NH_2), 3.91 (s, 3H, OCH_3). ^{13}C NMR (75 MHz, DMSO–d_6) δ (ppm): 166.2 (*C*=O), 143.7 (C), 142.4 (C), 139.5 (C), 132.1 (CH), 130.7 (C), 130.0 (CH), 129.2 (CH), 127.6 (CH–2 and CH–6 or CH–3 and CH–5), 126.7 (CH–2 and CH–6 or CH–3 and CH–5), 52.3 (O*C*H_3). MS (EI) *m/z* (%): 291 (100, $[M]^+$), 260 (71, $[M]^+ - OCH_3$), 152 (73). HRMS (EI) calcd for $C_{14}H_{13}NO_4S$ $[M]^+$ 291.0565. Found 291.0570. Anal. Calcd for $C_{14}H_{13}NO_4S$: C, 57.72; H, 4.50; N, 4.81; S, 11.01. Found: C, 57.46; H, 4.51; N, 4.85; S, 10.91.

4–(3–aminophenyl)benzenesulfonamide (4g). Brown solid, 94%. mp: 231 °C. ν_{max} (KBr) / cm^{-1}: 3385 (s) (NH_2), 3341 (SO_2NH_2), 3302 (CH), 1323 (s) (SO_2NH_2), 1158 (s) (SO_2NH_2), 1096. ^1H NMR (300 MHz, DMSO–d_6) δ (ppm): 7.89 (d, J = 8.4 Hz, 2H, H–2 and H–6 or H–3 and H–5), 7.75 (d, J = 8.4 Hz, 2H, H–2 and H–6 or H–3 and H–5), 7.40 (s, 2H, SO_2NH_2), 7.15 (t, J = 7.8 Hz, 1H), 6.90 (s, 1H, H–2′), 6.85 (d, J = 7.8 Hz, 1H), 6.64 (dd, J = 7.8, 1.2 Hz, 1H), 5.25 (s, 2H, NH_2). ^{13}C NMR (75 MHz, DMSO–d_6) δ (ppm): 149.5 (C–NH_2), 144.6 (C), 142.8 (C), 139.7 (C), 129.8 (CH), 127.1 (CH–2 and CH–6 or CH–3 and CH–5), 126.4 (CH–2 and CH–6 or CH–3 and CH–5), 114.7 (CH), 114.1 (CH), 112.4 (CH). MS (EI) *m/z* (%): 248 (100, $[M]^+$), 168 (45, $[M]^+ - SO_2NH_2$). HRMS (EI) calcd for $C_{12}H_{12}N_2O_2S$ $[M]^+$ 248.0619. Found 248.0624. Anal. Calcd for $C_{12}H_{12}N_2O_2S$: C, 58.05; H, 4.87; N, 11.28; S, 12.91. Found: C, 57.70; H, 4.89; N, 11.38; S, 12.74.

4–(4–aminophenyl)benzenesulfonamide (4h). Yellow solid, 98%. mp: 266 °C. ν_{max} (KBr) / cm^{-1}: 3426 (s) (NH_2), 3339 (SO_2NH_2), 3286 (CH), 1326 (s) (SO_2NH_2), 1155 (s) (SO_2NH_2), 1096. ^1H NMR (300 MHz, DMSO–d_6) δ (ppm): 7.81 (d, J = 8.4 Hz, 2H, H–2 and H–6 or H–3 and H–5), 7.73 (d, J = 8.4 Hz, 2H, H–2 and H–6 or H–3 and H–5), 7.46 (d, J = 8.4 Hz, 2H, H–2′ and H–6′ or H–3′ and H–5′), 7.32 (s, 2H, SO_2NH_2), 6.67 (d, J = 8.4 Hz, 2H, H–2′ and H–6′ or H–3′ and H–5′), 5.42 (s, 2H, NH_2). ^{13}C NMR (75 MHz, DMSO–d_6) δ (ppm): 149.6 (*C*–NH_2), 144.1 (*C*–SO_2NH_2), 141.1 (C), 127.8 (2 × CH), 126.4 (2 × CH), 125.6 (C), 125.5 (2 × CH), 114.4 (CH–2′ and CH–6′ or CH–3′ and CH–5′). MS (EI) *m/z* (%): 248 (100, $[M]^+$), 168 (38, $[M]^+ - SO_2NH_2$). HRMS (EI) calcd for $C_{12}H_{12}N_2O_2S$ $[M]^+$ 248.0619. Found 248.0623. Anal. Calcd for $C_{12}H_{12}N_2O_2S$: C, 58.05; H, 4.87; N, 11.28; S, 12.91. Found: C, 57.70; H, 4.91; N, 11.48; S, 12.69.

4–(4–cyanophenyl)benzenesulfonamide (4i). White solid, 100%. mp: 181 °C. ν_{max} (KBr) / cm^{-1}: 3344 (SO_2NH_2), 3245 (CH), 2222 (s) (CN), 1326 (s) (SO_2NH_2), 1148 (s) (SO_2NH_2), 1091. ^1H NMR (300 MHz, DMSO–d_6) δ (ppm): 8.04–7.92 (m, 8H), 7.48 (s, 2H, SO_2NH_2). ^{13}C NMR (75 MHz, DMSO–d_6) δ (ppm): 144.3 (C), 143.4 (C), 141.6 (C), 133.2 (CH–2′ and CH–6′ or CH–3′ and CH–5′), 128.2 (2 × CH), 127.9 (2 × CH), 126.6 (2 × CH), 118.9 (*C*–CN), 111.1 (C–*C*N). MS (EI)

m/z (%): 258 (100, $[M]^+$), 178 (80, $[M]^+ - SO_2NH_2$), 151 (51). HRMS (EI) calcd for $C_{13}H_{10}N_2O_2S$ $[M]^+$ 258.0463. Found 258.0469. Anal. Calcd for $C_{13}H_{10}N_2O_2S$: C, 60.45; H, 3.90; N, 10.85; S, 12.41. Found: C, 60.09; H, 3.75; N, 10.78; S, 12.02.

4–{4–[(1*H*–pyrazol–1–yl)methyl]phenyl}benzenesulfonamide (4j). Yellow solid, 83%. mp: 233 °C. ν_{max} (KBr) / cm^{-1}: 3354 (SO_2NH_2), 3318 (CH), 1326 (s) (SO_2NH_2), 1153 (s) (SO_2NH_2), 1099. ^{1}H NMR (300 MHz, DMSO–d_6) δ (ppm): 7.93–7.83 (m, 5H), 7.72 (d, J = 8.2 Hz, 2H, H–2′ and H–6′ or H–3′ and H–5′), 7.50 (d, J = 1.9 Hz, 1H, H–3″ or H–5″), 7.42 (s, 2H, SO_2NH_2), 7.35 (d, J = 8.2 Hz, 2H, H–2′ and H–6′ or H–3′ and H–5′), 6.31 (t, J = 1.9 Hz, 1H, H–4″), 5.40 (s, 2H, CH_2). ^{13}C NMR (75 MHz, DMSO–d_6) δ (ppm): 143.2 (*C*–SO_2NH_2 and C), 139.3 (CH–3″ or CH–5″), 138.2 (C), 138.1 (C), 130.5 (CH–3″ or CH–5″), 128.4 (2 × CH), 127.4 (2 × CH), 127.3 (2 × CH), 126.5 (2 × CH), 105.8 (CH–4″), 54.4 (CH_2). MS (EI) *m/z* (%): 313 (82, $[M]^+$), 312 (100), 246 (68, $[M]^+ - C_3H_3N_2$), 233 (9, $[M]^+ - SO_2NH_2$), 165 (65). HRMS (EI) calcd for $C_{16}H_{15}N_3O_2S$ $[M]^+$ 313.0885. Found 313.0887. Anal. Calcd for $C_{16}H_{15}N_3O_2S$: C, 61.32; H, 4.82; N, 13.41; S, 10.23. Found: C, 60.99; H, 4.70; N, 13.21; S, 9.91.

4–(3,4,5–trimethoxyphenyl)benzenesulfonamide (4k). White solid, 85%. mp: 160 °C. ν_{max} (KBr) / cm^{-1}: 3313 (SO_2NH_2), 3230 (CH), 1326 (s) (SO_2NH_2), 1248 (s) (OCH_3), 1163 (s) (SO_2NH_2), 1122 (s). ^{1}H NMR (300 MHz, DMSO–d_6) δ (ppm): 7.94–7.85 (m, 4H, H–2, H–6, H–3 and H–5), 7.42 (s, 2H, SO_2NH_2), 7.01 (s, 2H, H–2′ and H–6′), 3.89 (s, 6H, OCH_3–3′ and OCH_3–5′), 3.71 (s, 3H, OCH_3–4′). ^{13}C NMR (75 MHz, DMSO–d_6) δ (ppm): 153.3 (*C*–3′–OCH_3 and *C*–5′–OCH_3), 143.5 (C), 142.8 (C), 137.8 (C), 134.4 (C), 127.2 (CH–2 and CH–6 or CH–3 and CH–5), 126.1 (CH–2 and CH–6 or CH–3 and CH–5), 104.4 (CH–2′ and CH–6′), 60.1 (C–4′–OCH_3), 56.0 (C–3′–OCH_3 and C–5′–OCH_3). MS (EI) *m/z* (%): 323 (100, $[M]^+$), 308 (78, $[M]^+ - CH_3$). HRMS (EI) calcd for $C_{15}H_{17}NO_5S$ $[M]^+$ 323.0827. Found 323.0843. Anal. Calcd for $C_{15}H_{17}NO_5S$: C, 55.71; H, 5.30; N, 4.33; S, 9.92. Found: C, 55.37; H, 5.29; N, 4.50; S, 9.77.

4–[4–(4–bromophenyl)phenyl]benzenesulfonamide (4l). Pale pink solid, 80%. mp: 330 °C. ν_{max} (KBr) / cm^{-1}: 3333 ($SO_2\mathit{NH_2}$), 3245 (CH), 1313 (s) ($\mathit{SO_2}NH_2$), 1158 (s) ($\mathit{SO_2}NH_2$), 1101, 801 (s) (C–Br). ^{1}H NMR (300 MHz, DMSO–d_6) δ (ppm): 7.99–7.80 (m, 8H), 7.76–7.67 (m, 4H), 7.45 (s, 2H, $SO_2N\mathit{H_2}$). ^{13}C NMR (75 MHz, DMSO–d_6) δ (ppm): 143.3 (C), 142.8 (C), 138.9 (C), 138.8 (C), 138.2 (C), 132.1 (2 × CH), 129.0 (2 × CH), 127.9 (2 × CH), 127.5 (2 × CH), 127.3 (2 × CH), 126.6 (2 × CH), 121.4 (*C*–Br). MS (EI) *m/z* (%): 389 (100, $[^{81Br}M]^+$), 387 (97, $[^{79Br}M]^+$), 344 (52), 342 (51), 309 (21, $[^{81Br}M]^+ - SO_2NH_2$), 307 (20, $[^{79Br}M]^+ - SO_2NH_2$), 228 (81), 226 (65). HRMS (EI) calcd for $C_{18}H_{14}NO_2S^{81}Br$ $[M]^+$ 386.9929. Found 386.9940. Anal. Calcd for $C_{18}H_{14}NO_2SBr$: C, 55.68; H, 3.63; N, 3.61; S, 8.26. Found: C, 55.31; H, 3.73; N, 3.30; S, 7.89.

[1,1′:4′,1″–terphenyl]–4,4″–disulfonamide (4m). White solid, 91%. mp: 333 °C. ν_{max} (KBr) / cm^{-1}: 3344 ($SO_2\mathit{NH_2}$), 3266 (CH), 1326 (s) ($\mathit{SO_2}NH_2$), 1150 (s) ($\mathit{SO_2}NH_2$), 1099. ^{1}H NMR (300 MHz, DMSO–d_6) δ (ppm): 8.01–7.88 (m, 12H), 7.46 (s, 4H, $SO_2N\mathit{H_2}$–4 and $SO_2N\mathit{H_2}$–4″). ^{13}C NMR (75 MHz, DMSO–d_6) δ (ppm): 143.4 (2 × C), 142.8 (2 × C), 138.7 (2 × C), 128.0 (4 × CH), 127.4 (4 × CH), 126.6 (4 × CH). MS (EI) *m/z* (%): 388 (100, $[M]^+$), 308 (27, $[M]^+ - SO_2NH_2$), 228 (41, $[M]^+ - 2 \times SO_2NH_2$). HRMS (EI) calcd for $C_{18}H_{16}N_2O_4S_2$ $[M]^+$ 388.0552. Found 388.0570. Anal. Calcd for $C_{18}H_{16}N_2O_4S_2$: C, 55.65; H, 4.15; N, 7.21; S, 16.51. Found: C, 55.63; H, 4.10; N, 6.89; S, 16.15.

[1,1′:3′,1″–terphenyl]–4,4″–disulfonamide (4n). White solid, 94%. mp: 310 °C. ν_{max} (KBr) / cm^{-1}: 3370 ($SO_2\mathit{NH_2}$), 3251 (CH), 1331, 1318 (s) ($\mathit{SO_2}NH_2$), 1145 (s) ($\mathit{SO_2}NH_2$), 1091. ^{1}H NMR (300 MHz, DMSO–d_6) δ (ppm): 8.07 (t, J = 1.6 Hz, 1H, H–2′), 8.03 (d, J = 8.5 Hz, 4H, H–2, H–6, H–2″ and H–6″ or H–3, H–5, H–3″ and H–5″), 7.94 (d, J = 8.5 Hz, 4H, H–2, H–6, H–2″ and H–6″ or H–3, H–5, H–3″ and H–5″), 7.82 (dd, J = 7.4, 1.6 Hz, 2H, H–4′ and H–6′), 7.67 (dd, J = 7.4, 1.6 Hz, 1H, H–5′), 7.45 (s, 4H, $SO_2N\mathit{H_2}$–4 and $SO_2N\mathit{H_2}$–4″). ^{13}C NMR (75 MHz, DMSO–d_6) δ (ppm): 143.4 (2 × C), 143.3 (2 × C), 139.8 (2 × C), 130.1 (CH–2′ or CH–5′), 127.7 (CH–2, CH–6, CH–2″

and CH–6″ or CH–3, CH–5, CH–3″ and CH–5″), 127.2 (CH–4′ and CH–6′), 126.5 (CH–2, CH–6, CH–2″ and CH–6″ or CH–3, CH–5, CH–3″ and CH–5″), 126.0 (CH–2′ or CH–5′). MS (EI) *m/z* (%): 388 (100, $[M]^+$), 308 (35, $[M]^+ - SO_2NH_2$), 228 (39, $[M]^+ - 2 \times SO_2NH_2$). HRMS (EI) calcd for $C_{18}H_{16}N_2O_4S_2$ $[M]^+$ 388.0552. Found 388.0557. Anal. Calcd for $C_{18}H_{16}N_2O_4S_2$: C, 55.65; H, 4.15; N, 7.21; S, 16.51. Found: C, 55.26; H, 4.22; N, 7.12; S, 16.16.

4–(3–pyridinyl)benzenesulfonamide (4o). Yellow solid, 67%. mp: 200 °C. ν_{max} (KBr) / cm^{-1}: 3297 (SO_2NH_2), 3127 (CH), 1334 (s) (SO_2NH_2), 1166 (s) (SO_2NH_2), 1093. ^{1}H NMR (300 MHz, DMSO–d_6) δ (ppm): 8.98 (d, *J* = 2.1 Hz, 1H, H–2′), 8.65 (dd, *J* = 4.8, 1.5 Hz, 1H, H–4′), 8.18 (ddd, *J* = 8.0, 2.1, 1.5 Hz, 1H, H–6′), 8.00–7.90 (m, 4H, H–2, H–6, H–3 and H–5), 7.56 (dd, *J* = 8.0, 4.8 Hz, 1H, H–5′), 7.47 (s, 2H, SO_2NH_2). ^{13}C NMR (75 MHz, DMSO–d_6) δ (ppm): 149.5 (CH–2′ or CH–4′), 148.1 (CH–2′ or CH–4′), 143.8 (*C*–SO_2NH_2), 140.5 (C–4), 134.7 (CH–5′ or CH–6′), 134.2 (C–1′), 127.7 (CH–2 and CH–6 or CH–3 and CH–5), 126.6 (CH–2 and CH–6 or CH–3 and CH–5), 124.2 (CH–5′ or CH–6′). MS (EI) *m/z* (%): 234 (100, $[M]^+$), 154 (79, $[M]^+ - SO_2NH_2$). HRMS (EI) calcd for $C_{11}H_{10}N_2O_2S$ $[M]^+$ 234.0463. Found 234.0470. Anal. Calcd for $C_{11}H_{10}N_2O_2S$: C, 56.39; H, 4.30; N, 11.96; S, 13.69. Found: C, 56.08; H, 4.23; N, 11.98; S, 13.38.

4–(3–quinolinyl)benzenesulfonamide (4p). White solid, 56%. mp: 247 °C. ν_{max} (KBr) / cm^{-1}: 3318 (SO_2NH_2), 3137 (CH), 1328 (s) (SO_2NH_2), 1163 (s) (SO_2NH_2), 1096. ^{1}H NMR (300 MHz, DMSO–d_6) δ (ppm): 9.33 (d, *J* = 2.1 Hz, 1H, H–2′), 8.78 (d, *J* = 2.1 Hz, 1H, H–4′), 8.13 (d, *J* = 8.3 Hz, 2H, H–2 and H–6 or H–3 and H–5), 8.11 (d, *J* = 7.3 Hz, 2H, H–5′ and H–8′), 8.00 (d, *J* = 8.3 Hz, 2H, H–2 and H–6 or H–3 and H–5), 7.84 (td, *J* = 7.3, 1.0 Hz, 1H, H–6′ or H–7′), 7.70 (td, *J* = 7.3, 1.0 Hz, 1H, H–6′ or H–7′), 7.49 (s, 2H, SO_2NH_2). ^{13}C NMR (75 MHz, DMSO–d_6) δ (ppm): 149.5 (CH–2′), 147.3 (C–8′a), 143.8 (*C*–SO_2NH_2), 140.5 (C), 133.9 (CH), 131.6 (C), 130.3 (CH), 128.9 (CH), 128.8 (CH), 127.9 (CH–2 and CH–6 or CH–3 and CH–5), 127.7 (C), 127.4 (CH), 126.7 (CH–2 and CH–6 or CH–3 and CH–5). MS (EI) *m/z* (%): 284 (100, $[M]^+$), 204 (62, $[M]^+$ –

SO_2NH_2). HRMS (EI) calcd for $C_{15}H_{12}N_2O_2S$ $[M]^+$ 284.0619. Found 284.0626. Anal. Calcd for $C_{15}H_{12}N_2O_2S$: C, 63.36; H, 4.25; N, 9.85; S, 11.28. Found: C, 62.95; H, 4.31; N, 9.70; S, 10.90.

4–(1*H*–indol–5–yl)benzenesulfonamide (4q). Beige solid, 83%. mp: 248 °C. ν_{max} (KBr) / cm^{-1}: 3421 (s) (NH–1'), 3328 (SO_2NH_2), 3230 (CH), 1323 (s) (SO_2NH_2), 1313 (s), 1142 (s) (SO_2NH_2), 1093. ^{1}H NMR (300 MHz, DMSO–d_6) δ (ppm): 11.26 (NH–1'), 7.99–7.83 (m, 5H), 7.57–7.40 (m, 3H), 7.39 (s, 2H, SO_2NH_2), 6.54 (s, 1H, H–4′). ^{13}C NMR (75 MHz, DMSO–d_6) δ (ppm): 145.4 (C–7′a), 141.9 (*C*–SO_2NH_2), 136.2 (C), 130.0 (C), 128.5 (C), 127.1 (CH–2 and CH–6 or CH–3 and CH–5), 126.7 (CH), 126.5 (CH–2 and CH–6 or CH–3 and CH–5), 120.6 (CH), 119.0 (CH), 112.2 (CH–7′), 102.0 (CH–2′ or CH–3′). MS (EI) *m/z* (%): 272 (100, $[M]^+$), 192 (36, $[M]^+ - SO_2NH_2$). HRMS (EI) calcd for $C_{14}H_{12}N_2O_2S$ $[M]^+$ 272.0619. Found 272.0621. Anal. Calcd for $C_{14}H_{12}N_2O_2S$: C, 61.75; H, 4.44; N, 10.29; S, 11.77. Found: C, 61.38; H, 4.32; N, 10.21; S, 11.47.

4–(5–benzo[*d*][1,3]dioxolyl)benzenesulfonamide (4r). White solid, 100%. mp: 226 °C. ν_{max} (KBr) / cm^{-1}: 3333 (SO_2NH_2), 3259 (CH), 1320 (s) (SO_2NH_2), 1230 (OCH_2), 1155 (s) (SO_2NH_2), 1096. ^{1}H NMR (300 MHz, DMSO–d_6) δ (ppm): 7.89–7.79 (m, 4H, H–2, H–6, H–3 and H–5), 7.40 (s, 2H, SO_2NH_2), 7.36 (d, J = 1.7 Hz, 1H, H–4′), 7.26 (dd, J = 8.1, 1.7 Hz, 1H, H–6′), 7.06 (d, J = 8.1, Hz, 1H, H–7′), 6.10 (s, 2H, CH_2). ^{13}C NMR (75 MHz, DMSO–d_6) δ (ppm): 148.4 (*C*–O–1′ or *C*–O–3′), 147.8 (*C*–O–1′ or *C*–O–3′), 143.2 (C), 142.6 (C), 133.0 (C), 127.0 (CH–2 and CH–6 or CH–3 and CH–5), 126.4 (CH–2 and CH–6 or CH–3 and CH–5), 121.1 (CH), 109.0 (CH), 107.6 (CH), 101.6 (CH_2). MS (EI) *m/z* (%): 277 (100, $[M]^+$), 197 (36, $[M]^+ - SO_2NH_2$), 139 (51). HRMS (EI) calcd for $C_{13}H_{11}N_2O_4S$ $[M]^+$ 277.0409. Found 277.0407. Anal. Calcd for $C_{13}H_{11}N_2O_4S$: C, 56.31; H, 4.00; N, 5.05; S, 11.56. Found: C, 55.94; H, 3.97; N, 5.11; S, 11.36.

4–(1–phenylsulfonyl–1*H*–indol–3–yl)benzenesulfonamide (4s). White solid, 90%. mp: 219 °C. ν_{max} (KBr) / cm^{-1}: 3359 (SO_2NH_2), 3256 (CH), 1326 (s) (SO_2NH_2), 1168 (s) (SO_2Ph), 1160 (s) (SO_2NH_2), 1132 (s) (SO_2Ph), 1088. ^{1}H NMR (300 MHz, DMSO–d_6) δ (ppm): 8.31 (s, 1H, H–2'), 8.18–8.03 (m, 3H), 8.02–7.87 (m, 5H), 7.78–7.58 (m, 3H), 7.53–7.34 (m, 2H), 7.46 (s, 2H,

SO_2NH_2). ^{13}C NMR (75 MHz, DMSO–d_6) δ (ppm): 143.1 (*C*–SO_2NH_2), 137.0 (C), 136.0 (C), 135.1 (CH, C), 134.9 (C), 130.2 (2 × CH), 128.2 (2 × CH), 127.2 (2 × CH), 126.5 (2 × CH), 125.6 (CH), 125.1 (CH), 124.4 (CH), 121.8 (C), 120.6 (CH), 113.7 (CH–7'). MS (EI) *m/z* (%): 412 (65, $[M]^+$), 271 (100, $[M]^+$ – SO_2Ph). HRMS (EI) calcd for $C_{20}H_{16}N_2O_4S_2$ $[M]^+$ 412.0552. Found 412.0537. Anal. Calcd for $C_{20}H_{16}N_2O_4S_2$: C, 58.24; H, 3.91; N, 6.79; S, 15.55. Found: C, 57.93; H, 3.91; N, 6.63; S, 15.20.

4–(1–phenylsulfonyl–1*H*–indol–2–yl)benzenesulfonamide (4t). White solid, 79%. mp: 178 °C. ν_{max} (KBr) / cm^{-1}: 3364 (SO_2NH_2), 3251 (CH), 1383 (s) (SO_2Ph), 1305 (s) (SO_2NH_2), 1184 (s) (SO_2Ph), 1161 (s) (SO_2NH_2), 1088. ^1H NMR (300 MHz, DMSO–d_6) δ (ppm): 8.15 (d, *J* = 8.3 Hz, 1H), 7.94 (d, *J* = 8.2 Hz, 2H, H–2 and H–6 or H–3 and H–5), 7.80 (d, *J* = 8.2 Hz, 2H, H–2 and H–6 or H–3 and H–5), 7.66–7.39 (m, 7H), 7.44 (s, 2H, SO_2NH_2), 7.37–7.28 (m, 1H), 7.00 (s, 1H, H–3′). ^{13}C NMR (75 MHz, DMSO–d_6) δ (ppm): 144.0 (*C*–SO_2NH_2), 140.5 (C), 137.9 (C), 135.8 (C), 135.5 (C), 134.7 (CH), 130.5 (C), 130.4 (2 × CH), 129.6 (2 × CH), 126.5 (2 × CH), 125.8 (CH), 125.3 (2 × CH), 125.2 (CH), 121.7 (CH), 116.3 (CH–3′ or CH–7′), 116.0 (CH–3′ or CH–7′). MS (EI) *m/z* (%): 412 (78, $[M]^+$), 271 (100, $[M]^+$ – SO_2Ph), 191 (86), 110 (82). HRMS (EI) calcd for $C_{20}H_{16}N_2O_4S_2$ $[M]^+$ 412.0552. Found 412.0553. Anal. Calcd for $C_{20}H_{16}N_2O_4S_2$: C, 58.24; H, 3.91; N, 6.79; S, 15.55. Found: C, 57.91; H, 3.90; N, 6.65; S, 15.32.

4–(1*H*–indol–2–yl)benzenesulfonamide (4u). White solid, 60%. mp: 302 °C. ν_{max} (KBr) / cm^{-1}: 3431 (s) (NH–1'), 3339 (SO_2NH_2), 3251 (CH), 1297 (s) (SO_2NH_2), 1161 (s) (SO_2NH_2), 1096. ^1H NMR (300 MHz, DMSO–d_6) δ (ppm): 11.71 (s, 1H, NH–1′), 8.05 (d, *J* = 8.5 Hz, 2H, H–2 and H–6 or H–3 and H–5), 7.89 (d, *J* = 8.5 Hz, 2H, H–2 and H–6 or H–3 and H–5), 7.59 (d, *J* = 7.9 Hz, 1H, H–4′ or H–7′), 7.44 (d, *J* = 7.9 Hz, 1H, H–4′ or H–7′), 7.40 (s, 2H, SO_2NH_2), 7.16 (td, *J* = 7.9, 1.7 Hz, 1H, H–5′ or H–6′), 7.08 (d, *J* = 1.7 Hz, 1H, H–3′), 7.04 (t, *J* = 7.9 Hz, 1H, H–5′ or H–6′). ^{13}C NMR (75 MHz, DMSO–d_6) δ (ppm): 142.6 (*C*–SO_2NH_2), 137.7 (C), 136.2 (C), 135.5 (C), 128.6 (C), 126.5 (2 × CH), 125.3 (2 × CH), 122.6 (CH), 120.7 (CH), 119.9 (CH), 111.7 (CH–7′), 100.9

(CH). MS (EI) *m/z* (%): 272 (100, $[M]^+$), 192 (41, $[M]^+ - SO_2NH_2$). HRMS (EI) calcd for $C_{14}H_{12}N_2O_2S$ $[M]^+$ 272.0619. Found 272.0626. Anal. Calcd for $C_{14}H_{12}N_2O_2S$: C, 61.75; H, 4.44; N, 10.29; S, 11.77. Found: C, 61.51; H, 4.43; N, 10.16; S, 11.41.

4–(5–methoxy–1*H*–indol–2–yl)benzenesulfonamide (4v). White solid, 61%. mp: 265 °C. ν_{max} (KBr) / cm^{-1}: 3364 (s) (NH–1′), 3339 (SO_2NH_2), 3235 (CH), 1326 (s) (SO_2NH_2), 1220 (s) (OCH_3), 1155 (s) (SO_2NH_2), 1093. ^{1}H NMR (300 MHz, DMSO–d_6) δ (ppm): 11.55 (s, 1H, NH–1′), 8.02 (d, J = 8.4 Hz, 2H, H–2 and H–6 or H–3 and H–5), 7.88 (d, J = 8.4 Hz, 2H, H–2 and H–6 or H–3 and H–5), 7.39 (s, 2H, SO_2NH_2), 7.33 (d, J = 8.8 Hz, 1H, H–7′), 7.07 (d, J = 2.3 Hz, 1H, H–4′), 6.99 (s, 1H, H–3′), 6.81 (dd, J = 8.8, 2.3 Hz, 1H, H–6′), 3.78 (s, 3H, OCH_3). ^{13}C NMR (75 MHz, DMSO–d_6) δ (ppm): 154.0 (*C*–OCH_3), 142.4 (*C*–SO_2NH_2), 136.6 (C), 135.6 (C), 132.9 (C), 129.0 (C), 126.5 (CH–2 and CH–6 or CH–3 and CH–5), 125.1 (CH–2 and CH–6 or CH–3 and CH–5), 113.1 (CH), 112.5 (CH), 101.8 (CH), 100.7 (CH), 55.4 (OCH_3). MS (EI) *m/z* (%): 302 (100, $[M]^+$), 287 (44, $[M]^+ - CH_3$). HRMS (EI) calcd for $C_{15}H_{14}N_2O_3S$ $[M]^+$ 302.0725. Found 302.0733. Anal. Calcd for $C_{15}H_{14}N_2O_3S$: C, 59.59; H, 4.67; N, 9.27; S, 10.61. Found: C, 59.19; H, 4.63; N, 9.38; S, 10.34.

4–(2–benzo[*b*]furanyl)benzenesulfonamide (4w). White solid, 83%. mp: 272 °C. ν_{max} (KBr) / cm^{-1}: 3339 (SO_2NH_2), 3261 (CH), 1291 (s) (SO_2NH_2), 1155 (s) (SO_2NH_2), 1099. ^{1}H NMR (300 MHz, DMSO–d_6) δ (ppm): 8.13 (d, J = 8.4 Hz, 2H, H–2 and H–6 or H–3 and H–5), 7.95 (d, J = 8.4 Hz, 2H, H–2 and H–6 or H–3 and H–5), 7.73 (d, J = 7.5 Hz, 1H, H–4′ or H–7′), 7.69 (d, J = 7.5 Hz, 1H, H–4′ or H–7′), 7.65 (s, 1H, H–3′), 7.47 (s, 2H, SO_2NH_2), 7.40 (td, J = 7.5, 1.2 Hz, 1H, H–5′ or H–6′), 7.32 (t, J = 7.5 Hz, 1H, H–5′ or H–6′). ^{13}C NMR (75 MHz, DMSO–d_6) δ (ppm): 154.7 (C–2′ or C–7′a), 153.9 (C–2′ or C–7a′), 144.0 (*C*–SO_2NH_2), 132.8 (C), 128.8 (C), 126.7 (CH–2 and CH–6 or CH–3 and CH–5), 125.6 (CH), 125.2 (CH–2 and CH–6 or CH–3 and CH–5), 123.7 (CH), 121.8 (CH), 111.5 (CH), 104.5 (CH). MS (EI) *m/z* (%): 273 (100, $[M]^+$), 193 (25, $[M]^+ - SO_2NH_2$),

165 (44). HRMS (EI) calcd for $C_{14}H_{11}NO_3S$ $[M]^+$ 273.0460. Found 273.0458. Anal. Calcd for $C_{14}H_{11}NO_3S$: C, 61.52; H, 4.06; N, 5.12; S, 11.73. Found: C, 61.28; H, 4.03; N, 5.15; S, 11.72.

4–(2–benzo[*b*]thienyl)benzenesulfonamide (4x). White solid, 87%. mp: 314 °C. ν_{max} (KBr) / cm^{-1}: 3344 (SO_2NH_2), 3245 (CH), 1308 (s) (SO_2NH_2), 1163 (s) (SO_2NH_2), 1096. ^{1}H NMR (300 MHz, DMSO–d_6) δ (ppm): 8.09–7.97 (m, 4H), 7.93 (d, J = 8.4 Hz, 2H, H–2 and H–6 or H–3 and H–5), 7.91 (s, 1H, H–3′), 7.48 (s, 2H, SO_2NH_2), 7.46–7.39 (m, 2H). ^{13}C NMR (75 MHz, DMSO–d_6) δ (ppm): 143.8 (C), 141.7 (C), 140.5 (C), 139.2 (C), 136.8 (C), 126.8 (CH–2 and CH–6 or CH–3 and CH–5), 126.6 (CH–2 and CH–6 or CH–3 and CH–5), 125.5 (CH), 125.3 (CH), 124.4 (CH), 122.8 (CH), 122.2 (CH). MS (EI) *m/z* (%): 289 (100, $[M]^+$), 209 (32, $[M]^+ - SO_2NH_2$). HRMS (EI) calcd for $C_{14}H_{11}NO_2S_2$ $[M]^+$ 289.0231. Found 289.0231. Anal. Calcd for $C_{14}H_{11}NO_2S_2$: C, 58.11; H, 3.83; N, 4.84; S, 22.16. Found: C, 57.83; H, 3.60; N, 4.72; S, 22.56.

CA Inhibition Assay

An Applied Photophysics stopped–flow instrument has been used for assaying the CA catalyzed CO_2 hydration activity.[46] Phenol red (at a concentration of 0.2 mM) has been used as indicator, working at the absorbance maximum of 557 nm, with 10 mM Hepes (pH 7.4), 10 mM Tris·HCl and 0.1 M $NaSO_4$ (for maintaining constant the ionic strength), following the initial rates of the CA–catalyzed CO_2 hydration reaction for a period of 10–100 s. The CO_2 concentrations ranged from 1.7 to 17 mM for the determination of the kinetic parameters and inhibition constants. For each inhibitor, at least six traces of the initial 5–10% of the reaction have been used for determining the initial velocity. The non–catalyzed rates were determined in the same manner and subtracted from the total observed rates. Stock solutions of inhibitor (10 mM) were prepared in distilled–deionized water and dilutions up to 0.01 nM were done thereafter with distilled–deionized water. Inhibitor and enzyme solutions were pre–incubated together for 15 minutes at room temperature prior to assay, in order to allow for the formation of the E–I complex. The inhibition

constants were obtained by non−linear least−squares methods using PRISM 3, whereas the kinetic parameters for the uninhibited enzymes from Lineweaver−Burk plots, as reported earlier[46] and represent the mean from at least three different determinations. All CAs were recombinant proteins obtained as reported earlier by these groups.[44,45,47]

Co−crystallization and X−ray data collection

Crystals of hCA II complexed with compounds **4c**, **4g** and **4h** were obtained using the sitting drop vapor diffusion method. An equal volume of 0.8 mM solution of hCA II in Tris pH 8.0 and 1.6 mM of the inhibitors in Hepes 20 mM pH 7.4 was mixed and incubated for 15 minutes. 2 µL of the complex solution were mixed with 2 µL of a solution of 1.6 M sodium citrate, 50 mM Tris pH 8.0 and were equilibrated against the same solution at 296 K. Crystals of the complex grew in a few days. The crystals were flash−frozen at 100 K using a solution obtained by adding 25% (v/v) glycerol to the mother liquor solution as cryoprotectant. Data on crystals of the complexes were collected using synchrotron radiation at the BM30A beamline at ESRF (Grenoble, France) with a wavelength of 0.980 Å and an ADSC Q315r CCD detector. Data were integrated and scaled using the program XDS.[48] Data processing statistics are showed in the Supporting Information, Table S2.

Structure determination

The crystal structure of hCA II (PDB accession code: 4FIK) without solvent molecules and other heteroatoms was used to obtain initial phases of the structures using Refmac5.[49] 5% of the unique reflections were selected randomly and excluded from the refinement data set for the purpose of Rfree calculations. The initial |Fo − Fc| difference electron density maps unambiguously showed the inhibitor molecules. An electron density, which could be interpreted as a second molecule of inhibitor **4g,** was present near the *N*−terminal region of the protein. Thus, a second **4g** molecule was introduced in the model and refined with unitary occupancy. Moreover, after the introduction of molecule **4c**, residual electron densities were present in the Fo − Fc map and they were interpreted

as water molecules at partial occupancy. Also, a partial occupancy was assigned to the atoms of compound **4c**. Atomic models for inhibitors were calculated and the energy minimized using the program JLigand 1.0.39. Refinements proceeded using normal protocols of positional, isotropic atomic displacement parameters alternating with manual building of the models using COOT.[50] Solvent molecules were introduced automatically using the program ARP.[51] The quality of the final models were assessed with COOT and Rampage.[52] Crystal parameters and refinement data are summarized in the Supporting Information, Table S2. Atomic coordinates were deposited in the Protein Data Bank (PDB accession code: 5E28, 5E2K, 5E2S). Graphical representations were generated with Chimera.[53]

Acknowledgements

BC is grateful for financial support from Italian Ministry of Education, University and Research (MIUR, PRIN 2010−2011 − prot. 2010N3T9M4), Italian−French University (Vinci 2011), University of Chieti−Pescara, "Centre National de la Recherche Scientifique (CNRS)" and the University of Reims. GAR and ANK are grateful to the European Research Council (ERC) for financial support and to the Nottingham Nanotechnology and Nanoscience Centre (NNNC) for access to transmission electron microscopy facilities. NMR spectroscopic measurements by C. Petermann, MS spectrometric measurements by C. Machado and elemental analysis measurements by S. Lathony (University of Reims) are gratefully acknowledged. MF thanks the staff of beamline BM30A of the European Synchrotron Radiation Facility (Grenoble, France) for technical assistance during data collection.

References

(1) Del Prete, S.; Vullo, D.; Ficher, G. M.; Andrews, K. T.; Poulsen S.−A.; Capasso, C.; Supuran C. T. Discovery of a new family of carbonic anhydrases in the malaria pathogen *Plasmodium falciparum*− the $\eta-$carbonic anhydrases. *Bioorg. Med. Chem. Lett.* **2014**, *24*, 4389−4396.

(2) Krishnamurthy, V. M.; Kaufman, G. K.; Urbach, A. M.; Gitlin, I.; Gudiksen, K. L.; Weibel, D. B.; Whitesides, G. M. Carbonic anhydrase as a model for biophysical and physical–organic studies of proteins and protein–ligand binding. *Chem. Rev.* **2008**, *108*, 946–1051.

(3) Supuran, C. T. Carbonic anhydrases: novel therapeutic applications for inhibitors and activators. *Nat. Rev. Drug. Discovery* **2008**, *7*, 168–181.

(4) Alterio, V.; Di Fiore, A.; D'Ambrosio, K.; Supuran, C. T.; De Simone, G. Multiple binding modes of inhibitors to carbonic anhydrases: how to design specific drugs targeting 15 different isoforms? *Chem. Rev.* **2012**, *112*, 4421–4468.

(5) Neri, D.; Supuran, C. T. Interfering with pH regulation in tumors as a therapeutic strategy. *Nat. Rev. Drug Discovery* **2011**, *10*, 767–777.

(6) Supuran, C. T. Carbonic anhydrase inhibitors and activators for novel therapeutic applications. *Future Med. Chem.* **2011**, *3*, 1165–1180.

(7) Supuran, C. T.; Casini, A.; Scozzafava, A. In *Carbonic anhydrase: Its inhibitors and activators*; Supuran, C. T., Scozzafava, A., Conway, J., Eds.; CRC Press: Boca Raton, FL, 2004; p 67.

(8) Supuran, C. T. In *Drug Design of Zinc–Enzyme Inhibitors: Functional, Structural, and Disease Applications*; Supuran, C. T., Winum, J. Y., Eds.; Wiley: Hoboken (NJ), 2009; pp 15–38.

(9) Aggarwal, M.; Kondeti, B.; McKenna, R. Anticonvulsivant/antiepileptic carbonic anhydrase inhibitors: a patent review. *Expert Opin. Ther. Pat.* **2013**, *23*, 717–724.

(10) Temperini, C.; Scozzafava, A. In *Drug Design of Zinc–Enzyme Inhibitors: Functional, Structural, and Disease Applications*; Supuran, C. T., Winum, J. Y., Eds.; Wiley: Hoboken (NJ), 2009; p 473.

(11) Ratto, F.; Witort, E.; Tatini, F.; Centi, S.; Lazzeri, L.; Carta, F.; Lulli, M.; Vullo, D.; Fusi, F.; Supuran, C. T.; Scozzafava, A.; Capaccioli, S.; Pini, R. Plasmonic particles that hit hypoxic cells. *Adv. Func. Mater.* **2015**, *25*, 316–323.

(12) Dilworth, J. R.; Pascu, S. I.; Waghorn, P. A.; Vullo, D.; Bayly, S. R.; Christlieb, M.; Sun, X.; Supuran, C. T. Synthesis of sulfonamide conjugates of Cu(II), Ga(III), In(III), Re(V) and Zn(II) complexes: carbonic anhydrase inhibition studies and cellular imaging investigations. *Dalton Trans.* **2015**, *44*, 4859–4873.

(13) De Simone, G.; Alterio, V.; Supuran, C. T. Exploiting the hydrophobic and hydrophilic binding sites for designing carbonic anhydrase inhibitors. *Expert Opin. Drug Discov.* **2013**, *8*, 793–810.

(14) Weber, A.; Casini, A.; Heine, A.; Kuhn, D.; Supuran, C. T.; Scozzafava, A.; Klebe, G. Unexpected nanomolar inhibition of carbonic anhydrase by COX–2 selective Celecoxib: New pharmacological opportunities due to related binding site recognition. *J. Med. Chem.* **2004**, *47*, 550–557.

(15) Carta, F.; Aggarwal, M.; Maresca, A.; Scozzafava, A.; McKenna, R.; Supuran, C. T. Dithiocarbamates: a new class of carbonic anhydrase inhibitors. Crystallographic and kinetic investigations. *Chem. Commun.* **2012**, *48*, 1868–1870.

(16) Almajan, G. L.; Innocenti, A.; Puccetti, L.; Manole, G.; Barbuceanu, S.; Saramet, I.; Scozzafava, A.; Supuran, C. T. Carbonic anhydrase inhibitors. Inhibition of the cytosolic and tumor–associated carbonic anhydrase isozymes I, II, and IX with a series of 1,3,4–thiadiazole– and 1,2,4–triazole–thiols. *Bioorg. Med. Chem. Lett.* **2005**, *15*, 2347–2352.

(17) Di Fiore, A.; Maresca, A.; Supuran, C. T.; De Simone, G. Hydroxamate represents a versatile zinc binding group for the development of new carbonic anhydrase inhibitors. *Chem. Commun.* **2012**, *48*, 8838–8840.

(18) Carta, F.; Vullo, D.; Maresca, A.; Scozzafava, A.; Supuran, C. T. Mono–/dihydroxybenzoic acid esters and phenol pyridinium derivatives as inhibitors of the mammalian carbonic anhydrase isoforms I, II, VII, IX, XII and XIV. *Bioorg. Med. Chem.* **2013**, *21*, 1564–1569.

(19) Martin, D. P.; Cohen, S. M. Nucleophile recognition as an alternative inhibition mode for benzoic acid based carbonic anhydrase inhibitors. *Chem. Commun.* **2012**, *48*, 5259–5261.

(20) Carta, F.; Temperini, C.; Innocenti, A.; Scozzafava, A.; Kaila, K.; Supuran, C. T. Polyamines inhibit carbonic anhydrases by anchoring to the Zinc–coordinated water molecule. *J. Med. Chem.* **2010**, *53*, 5511–5522.

(21) Davis, R. A.; Hofmann, A.; Osman, A.; Hall, R. A.; Mühlschlegel, F. A.; Vullo, D.; Innocenti, A.; Supuran, C. T.; Poulsen, S.–A. Natural product–based phenols as novel probes for mycobacterial and fungal carbonic anhydrases. *J. Med. Chem.* **2011**, *54*, 1682–1692.

(22) Tars, K.; Vullo, D.; Kazaks, A.; Leitans, J.; Lends, A.; Grandane, A.; Zalubovskis, R.; Scozzafava, A.; Supuran, C. T. Sulfocumarins (1,2–benzoxathiine–2,2–dioxides): a class of potent and isoform–selective inhibitors of tumor–associated carbonic anhydrases. *J. Med. Chem.* **2013**, *56*, 293–300.

(23) Maresca, A.; Temperini, C.; Vu, H.; Pham, N. B.; Poulsen, S.–A.; Scozzafava, A.; Quinn, R. J.; Supuran, C. T. Non–Zinc mediated inhibition of carbonic anhydrases: cumarins are a new class of suicide inhibitors. *J. Am. Chem. Soc.* **2009**, *131*, 3057–3062.

(24) Touisni, N.; Maresca, A.; McDonald, P. C.; Lou, Y.; Scozzafava, A.; Dedhar, S.; Winum, J.–Y.; Supuran, C. T. Glycosyl cumarin carbonic anhydrase IX and XII inhibitors strongly attenuate the growth of primary breast tumors. *J. Med. Chem.* **2011**, *54*, 8271–8277.

(25) Mann, T.; Keilin, D. Sulphanilamide as a specific inhibitor of carbonic anhydrase. *Nature* **1940**, *146*, 164–165.

(26) Ceruso, M.; Antel, S.; Scozzafava, A.; Supuran, C. T. Synthesis and inhibition potency of novel ureido benzenesulfonamides incorporating GABA as tumor–associated carbonic anhydrase IX and XII inhibitors. *J. Enzyme Inhib. Med. Chem.* **2015**, *20*, 1–7.

(27) Alterio, V.; Di Fiore, A.; D'Ambrosio, K.; Supuran, C. T.; De Simone, G. In *Drug Design of Zinc–Enzyme Inhibitors: Functional, Structural, and Disease Applications*; Supuran, C. T., Winum, J. Y., Eds.; Wiley: Hoboken (NJ), 2009; p 73.

(28) Di Fiore, A.; Maresca, A.; Alterio, V.; Supuran, C. T.; De Simone, G. Carbonic anhydrase inhibitors: X–ray crystallographic studies for the binding of *N*–substituted benzenesulfonamide to human isoform II. *Chem. Commun.* **2011**, *47*, 11636–11638.

(29) Rogez–Florent, T.; Meignan, S.; Foulon, C.; Six, P.; Gros, A.; Bal–Mahieu, C.; Supuran, C. T.; Scozzafava, A.; Frédérick, R.; Masereel, B.; Depreux, P.; Lansiaux, A.; Goossens, J.–F.; Gluszok, S.; Goossens, L. New selective carbonic anhydrase IX inhibitors: Synthesis and pharmacological evaluation of diarylpyrazole–benzenesulfonamides. *Bioorg. Med. Chem.* **2013**, *21*, 1451–1464.

(30) Compain, G.; Martin–Mingot, A.; Maresca, A.; Thibaudeau, S.; Supuran, C. T. Superacid synthesis of halogen containing *N*–substituted–4–aminobenzenesulfonamides: New selective tumor–associated carbonic anhydrase inhibitors. *Bioorg. Med. Chem.* **2013**, *21*, 1555–1563.

(31) Güzel–Akdemir, Ö.; Biswas, S.; Lastra, K.; McKenna, R.; Supuran, C. T. Structural study of the location of the phenyl tail of benzenesulfonamides and the effect on human carbonic anhydrase inhibition. *Bioorg. Med. Chem.* **2013**, *21*, 6674–6680.

(32) Mahon, B. P.; Pinard, M. A.; McKenna, R. Targeting carbonic anhydrase IX activity and expression. *Molecules* **2015**, *20*, 2323–2348.

(33) Alafeefy, A. M.; Isik, S.; Abdel–Aziz, H. A.; Ashour, A. E.; Vullo, D.; Al–Jaber, N. A.; Supuran, C. T. Carbonic anhydrase inhibitors: Benzenesulfonamides incorporating

cyanoacrylamide moieties are low nanomolar/subnanomolar inhibitors of the tumor–associated isoforms IX and XII. *Bioorg. Med. Chem.* **2013**, *21*, 1396–1403.

(34) Salmon, A. J.; Williams, M. L.; Wu, Q. K.; Morizzi, J.; Gregg, D.; Charman, S. A.; Vullo, D.; Supuran, C. T.; Poulsen S.–A. Metallocene–based inhibitors of cancer–associated carbonic anhydrase enzymes IX and XII. *J. Med. Chem.* **2012**, *55*, 5506–5517.

(35) Pala, N.; Micheletto, L.; Sechi, M.; Aggarwal, M.; Carta, F.; McKenna, R.; Supuran, C. T. Carbonic anhydrase inhibition with benzenesulfonamides and tetrafluorobenzenesulfonamides obtained via click chemistry. *ACS Med. Chem. Lett.* **2014**, *5*, 927–930.

(36) Bozdag, M.; Ferraroni, M.; Nuti, E.; Vullo, D.; Rossello, A.; Carta, F.; Scozzafava, A.; Supuran, C. T. Combining the tail and the ring approaches for obtaining potent and isoform–selective carbonic anhydrase inhibitors: Solution and X–ray crystallographic studies. *Bioorg. Med. Chem.* **2014**, *22*, 334–340.

(37) Ahlskog, J. K. J.; Durnelin, C. E.; Trüssel, S.; Marlind, J.; Neri, D. In vivo targeting of tumor–associated carbonic anhydrases using acetazolamide derivatives. *Bioorg. Med. Chem. Lett.* **2009**, *19*, 4851–4856.

(38) Miyaura, N.; Suzuki, A. Palladium–catalysed cross–coupling reactions of organoboron compounds. *Chem. Rev.* **1995**, *95*, 2457–2483.

(39) Billingsley, K.; Buchwald, S. Highly efficient monophosphine–based catalyst for the Palladium–catalysed Suzuki–Miyaura reaction of heteroaryl halides and heteroaryl boronic acids and esters. *J. Am. Chem. Soc.* **2007**, *129*, 3358–3366.

(40) Yasuda, N. Application of cross–coupling reactions in Merck. *J. Organomet. Chem.* **2002**, *653*, 279–287.

(41) Heravi. M. M.; Hashemi, E. Recent applications of the Suzuki reaction in total synthesis. *Tetrahedron* **2012**, *68*, 9145–9178.

(42) Desos, P.; Cordi, A.; Lestage, P. New phenyl−pyridinyl−piperazine derivatives as H_3 receptor antagonists, process for their preparation, and pharmaceutical compositions containing them (Les Laboratoires Servier) WO 2006/120349 A1. *Chem. Abstr*. *145*, 489280 (**2006**).

(43) Cornelio, B.; Rance, G. A.; Laronze−Cochard, M.; Fontana, A.; Sapi, J.; Khlobystov, A. N. Palladium nanoparticles on carbon nanotubes as catalysts of cross−coupling reactions. *J. Mater. Chem. A* **2013**, *1*, 8737−8744.

(44) Vullo, D.; Innocenti, A.; Nishimori, I.; Pastorek, J.; Scozzafava, A.; Pastorekova, S.; Supuran, C. T. Carbonic anhydrase inhibitors. Inhibition of the transmembrane isozyme XII with sulfonamides−a new target for the design of antitumor and antiglaucoma drugs? *Bioorg. Med. Chem. Lett*. **2005**, *15*, 963−969.

(45) D'Ambrosio, K.; Vitale, R. M.; Dogné, J. M.; Masereel, B.; Innocenti, A.; Scozzafava, A.; De Simone, G.; Supuran, C. T. Carbonic anhydrase inhibitors: bioreductive nitro−containing sulfonamides with selectivity for targeting the tumor associated isoforms IX and XII. *J. Med. Chem*. **2008,** *51*, 3230−3237.

(46) Khalifah, R. G. The carbon dioxide hydration activity of carbonic anhydrase I. Stop−flow kinetic studies on the native human isoenzymes B and C. *J. Biol. Chem*. **1971**, *246*, 2561−2573.

(47) Duda, D. M.; Tu, C.; Fisher, S. Z.; An, H.; Yoshioka, C.; Govindasamy, L.; Laipis, P. J.; Agbandje−McKenna, M.; Silverman, D. N.; McKenna, R. Human carbonic anhydrase III: structural and kinetic study of catalysis and proton transfer. *Biochemistry* **2005,** *44*, 10046−10053.

(48) Kabsch, W. Integration, scaling, space−group assignement and post refinement. *Acta Cryst.* **2010**, *D66*, 133−144.

(49) Murshudov, G. N.; Vagin, A. A.; Dodson, E. J. Refinement of macromolecular structures by the maximum−likelihood method. *Acta Cryst.* **1997**, *D53*, 240−255.

(50) Emsley, P.; Lohkamp, B.; Scott, W.; Cowtan, K. Features and development of coot, *Acta Cryst.* **2010**, *D66*, 486–501.

(51) Lamzin, V. S.; Perrakis, A.; Wilson, K. S. In *Int. Tables for Crystallography. Vol. F: Crystallography of biological macromolecules;* Rossmann, M. G., Arnold, E., Eds.; Dordrecht, Kluwer Academic Publishers, The Netherlands, 2001; p 720.

(52) Lovell, S. C.; Davis, I. W.; Arendall III W. B.; de Bakker, P. I. W.; Word, J. M.; Prisant, M. G.; Richardson, J. S.; Richardson D. C. Structure validation by Calpha geometry: phi,psi and Cbeta deviation. *Proteins* **2003**, *50*, 437–450.

(53) Pettersen, E. F.; Goddard, T. D.; Huang, C. C.; Couch, G. S.; Greenblatt, D. M.; Meng, E. C.; Ferrin, T. E. UCSF Chimera – a visualization system for exploratory research and analysis. *J. Comput. Chem.* **2004**, *25*, 1605–1612.

TOC Graphic